Using an Analytical Model to Design Liquid Crystal Microlenses

José Francisco Algorri, Virginia Urruchi, Noureddine Bennis,
and José Manuel Sánchez-Pena

***Abstract*— We have developed new analytical expressions for designing liquid crystal (LC) microlenses. These equations are based on a novel equivalent electric circuit and can be used to create an optimum design for the LC lenses in which the lens diameter ranges from a few micrometers to several millimeters. Thus far, only experimental studies have been conducted on the LC lenses. The analytical expressions developed in this letter depend on various manufacturing parameters and can be used to design lenses with specific focal lengths and a parabolic phase profile. The required driving scheme (modal or hole-patterned) can be predicted. The LC microlenses were manufactured and electrooptically characterized: the measurements were compared using an analytical approach.**

***Index Terms*— Liquid crystals devices, optoelectronic materials, micro-optics, advanced optics design.**

I. Introduction

LIQUID crystal (LC) lenses have been an important research field for many years. Recent research applications have spurred interest in mechanisms and new structures that exploit the typical anisotropy of LC mixtures for developing new functionalities. Some examples are tunable-focusing optical zoom systems, spectacles or autostereoscopic devices [1], [2]. Much of the effort that has been expended in studying these reported topologies has focused on reducing the number of control electrodes and the amplitude of the control voltage [3]. However, the practical restrictions on these devices have only been demonstrated experimentally, thus far. For example, at the micrometric scale, a modal control technique [4] has shown some constraints on fabrication, i.e., very high resistivity layers are required. However, hole-patterned LC lenses [5] are only functional for lenses with very small diameters.

In this letter, we develop an analytical approach to produce design equations for manufacturing LC microlenses. A useful protocol has been derived for this purpose. Transmission line theory is used to model the electrical response of the lenses. An equivalent electric circuit (EEC) is developed, which is a transmission line involving coplanar capacitances [6]. These capacitances describe the physical effect of the fringe field between electrodes that are placed on the same surface of a LC microlens. The manufacturing protocol is optimized to reduce aberrations from shrinkage and flatness effects and to obtain tunable lenses.

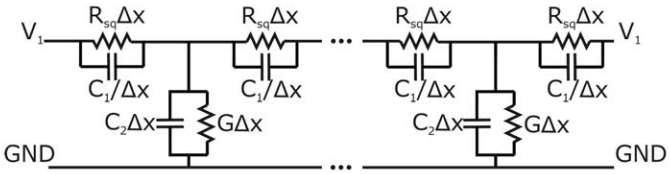

Fig. 1. Proposed EEC based on transmission line theory.

II. Analytical Expressions for Designing LC Microlenses

As commented above, a novel EEC has been developed to design LC microlenses [7]; it is shown in Fig. 1.

This scheme is a transmission line involving distributed capacitances and models the effect of the typical parasitic capacitances between the teeth of the comb electrode for LC microlenses. The resulting equation of this model is shown in (1). The denominator of this equation contains two key parameters.

$$\frac{\partial V^2(x)}{\partial x^2} = \frac{G + j \cdot \omega \cdot C_2}{1/R_{sq} + j \cdot \omega \cdot C_1} \cdot V(x) = \Psi \cdot V(x) \qquad (1)$$

These two parameters determine the topology required to fabricate a LC microlens. The relationship between the components of the EEC (C_1, C_2, R_{sq} and G) and the structural dimensions is taken from Ref. [7]. From impedance considerations, small-diameter lenses require very high resistivity layers; however, $|Z_{C1}|$ ($1/\omega C_1$) can be decreased up to a critical value at which a resistivity layer is no longer needed. In contrast, if the lens diameter is too large, the parameter $|Z_{C1}|$ becomes too high and can be neglected for a parallel topology. In the following sections, the structural requirements of a LC microlens are determined. The characteristics of the EEC depend on the $|Z_{C1}|$ and the resistance produced by R_{sq} (R).

a) Modal microlens without a parasitic capacitive effect, $R << |Z_{C1}|$: the EEC developed for this case is the simplest to apply and is valid for large diameters (>1mm)
b) Microlens with a complete EEC, $R < |Z_{C1}|$: in the most general case, the EEC exhibits both resistive

(R) and capacitive (C_1) effects; however, the resistive effect predominates

c) Modal limiting condition, $R = |Z_{C1}|$: the resistance and capacitance are comparable, resulting in a limiting condition

d) Hole-patterned microlens, $R >> |Z_{C1}|$: a specific thickness-diameter relationship causes the electrical field to distributed across the lens diameter.

A. Modal Microlens Without Parasitic Capacitive Effect

It is well known that the phase delay in a LC lens is nonlinearly related to the voltage distribution. To obtain a proper phase distribution for a symmetric microlens, i.e., to avoid undesirable shrinkage effects at the sides of the lens or a plateau in the center of the optical phase, the voltage at the electrode and the microlens center must equal the saturation voltage and the threshold voltage, respectively. Thus, we introduce a new parameter as follows:

$$\alpha = \alpha' + j\alpha'' = V_1/V_{x=0}. \tag{2}$$

As previously mentioned, this relationship depends on the LC characteristics. The imaginary part (2) corresponds to the electrical phase shift at the center of the lens. Two methods can be used to accurately estimate the modulus of this parameter. In the first and more accurate method, the LC birefringence is measured using spectroscopy. In the second method, the Frank-Oseen equations are simulated. If an external perturbation, such as an electrical field, is formally introduced into the system, the deformation of the molecular director can be estimated by minimizing the Gibbs free energy. Subsequently, this parameter is considered to be a known variable. Solving (1) with the boundary conditions $V_{-x} = V_x = V_1$ (where x denotes the lens radius) for one harmonic yields

$$V_{x=0} = V_1/cosh(\sqrt{\Psi}\cdot r) \;\Rightarrow \Psi = acosh^2(\alpha)/r^2. \tag{3}$$

In a nematic LC, the impedance, Z_{C2}, in the EEC is always smaller than the parallel conductance [8] G and can therefore be neglected (henceforth, the impedance in the EEC is suppressed). As we are not considering the parasitic capacitive effect (C_1), the sheet resistance of the resistivity layer is given as follows:

$$R_{sq} = \frac{1}{\frac{r^2 j\omega C_2}{acosh^2(\alpha)}} = \frac{d\cdot acosh^2(\alpha' + j\alpha'')}{r^2\left(\varepsilon_0\varepsilon'_2 j\omega\right)} \approx \frac{d\cdot 2acosh^2(|\alpha|)}{r^2\left(\varepsilon_0\varepsilon'_2\omega\right)}, \tag{4}$$

where d denotes the LC thickness, and ε'_2 denotes the LC real permittivity perpendicular to the glasses. An analytical approximation is obtained using hyperbolic trigonometric relations. In the resulting equivalence solution, a sinusoidal function ([−1, 1]) is suppressed due to a hyperbolic cosine component (exponential behavior). This approximation only produces significant errors for low values of $|\alpha|$ (Fig. 2).

The approximate solution was compared with the exact solution using a brute force algorithm. In this case, the error corresponds to the chosen tolerance. It is very important to estimate this resistance in the early stages of the design phase of LC lenses. Different materials and techniques have been developed to manufacture high resistivity layers for modal devices; however, only experimental studies have been conducted in the literature, thus far (to the best of our knowledge). Design at the micrometer scale is not a simple task and sometimes requires the use of very thin metallic layers with unusual physical properties [9]. Thus, (4) is an important design tool. The measured error is within the same range as those incurred in the manufacturing process and is not in itself a determining factor. In addition, the resistance is a frequency dependent parameter, such that the errors in the design estimates can be easily corrected. However, (4) shows that decreasing the diameter (2r) increases the sheet resistance quadratically. As previously mentioned, the critical value at which the impedance of the parasitic capacitor C_1 becomes smaller than the parallel resistance determines whether or not a high resistivity layer is required.

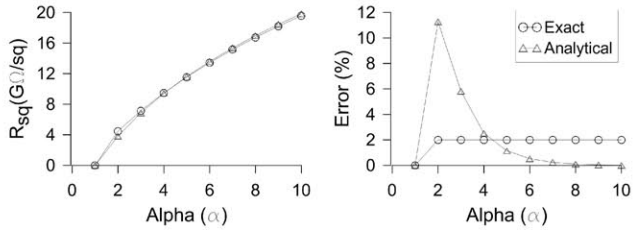

Fig. 2. Square resistance as a function of Alpha (α) for r = 285μm, d = 50μm and f = 1 kHz (left) and comparison of errors for the two techniques (right).

B. Microlens With Complete ECC

This general case is rarely encountered in practice, because an optimum design is only relevant for the modal or hole-patterned regime. For this reason, this case is not detailed in this letter.

C. Modal Limit

As previously mentioned, there is an important consideration in the design of LC microlenses. The required resistance increases when the diameter decreases, resulting in a critical value at which the capacitor C_1 produces a distributed electrical field, such that a high resistivity layer is not required. The modal limit corresponds to the resistance of the high resistivity layer being equal to the impedance modulus of the C_1 capacitor:

$$R = \frac{r}{l}R_{sq} = \frac{d\cdot 2\cdot acosh^2(|\alpha|)}{r\varepsilon_0\varepsilon'_2\omega l} \tag{5}$$

$$|Z_C 1| = \frac{1}{(l/r)\omega C_1} = \frac{r\cdot A}{\varepsilon_0\varepsilon'_1\omega l d}, \tag{6}$$

where r denotes the radius, l denotes the lens depth, ε'_1 and ε'_2 denote the LC real permittivity parallel and perpendicular to the glasses, respectively, and A is a parameter that depends on fringe field effects and is related to the dimensions of the electrode and the lens diameter. In the modal limit,

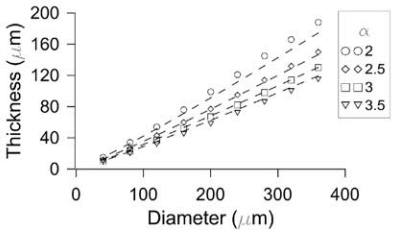

Fig. 3. Relationship between the thickness and the diameter for different gains (α): the FEM simulations are shown as symbols and (8) is shown as a dashed line.

the resistance from the high resistivity layer is equal to the capacitor impedance. The radius that corresponds to this limit is given below.

$$R = |Z_{C1}| \Rightarrow r_{CRIT} = d \cdot acosh(|\alpha|)\sqrt{\frac{2 \cdot \varepsilon_1'}{\varepsilon_2' \cdot A}}. \quad (7)$$

The exact solution of this formula requires that the molecular position be known. This position can be estimated using the Frank Oseen equations and an iterative algorithm. If the phase profile is a constant, the relation $\varepsilon_1/\varepsilon_2$ is also constant, and an approximate solution can be obtained. All of the molecules in the quadratic range of the birefringence are at a certain angle to each electrode thus, the mean molecular position is given by $\varepsilon'_1 = 0.7\Delta\varepsilon' + \varepsilon'_o$ and $\varepsilon'_2 = 0.3\Delta\varepsilon' + \varepsilon'_o$ [7]. A high resistivity layer is required when the lens radius is larger than r_{CRIT}. However, if the lens radius is smaller than r_{CRIT}, the LC impedance dominates the electrical gradient, and a high resistivity layer is not required for manufacturing the devices. In this case, a suitable gradient can be achieved using the fringe field effect if the thickness follows the relationship given in (11). Thus far, this relationship has only been investigated experimentally. In this letter, an analytical expression has been developed for the first time for the aforementioned relationship in terms of simple functions.

D. Hole-Patterned Microlens

As discussed above, (7) shows the limiting condition at which the resistance of the high resistivity layer equals the LC inherent impedance (Z_{C1}). Without a high resistivity layer, the voltage is distributed by the capacitor, C_1, thereby simplifying the ECC. Using (3), the thickness (d) can be related to the diameter (2r) as follows:

$$\Psi = \frac{C_2}{C_1} = \frac{\varepsilon_2'/d}{\varepsilon_1' d/A} \Rightarrow \frac{r}{d} = acosh\,(|\alpha|)\sqrt{\frac{\varepsilon_1'}{\varepsilon_2' \cdot A}}. \quad (8)$$

This equation is essential for LC microlens manufacture, because it provides the key dimensions required to design generating phase gradients similar to those in conventional lenses (without shrinkage or plateau defects). The results from (8) were compared (Fig. 3) with those obtained using the finite element method (FEM) to solve Poisson's equation from electrostatics:

$$\nabla \cdot (\varepsilon \nabla V) = \rho, \quad (9)$$

where ε is the anisotropic dielectric coefficient, and ρ is the space charge density (which is zero in this case).

The results of the developed equation are in fair agreement with the FEM estimates. This demonstrates that the component C_1 of the EEC is a good approximation to the fringe fields effects produced in this type of structures.

III. Microlens Design Protocol

The focal length has been identified as the main parameter for modeling a lens for most applications. LC lenses are GRIN (GRadient INdex) lenses; therefore, estimating their focal length, f_{GRIN}, can be simplified by considering the focusing of parallel rays:

$$f_{GRIN} = r^2/2d\Delta n. \quad (10)$$

The aforementioned parameter is associated with three adjustable variables: the diameter, the thickness and the difference between the maximum refractive index at the optical axis of each lens, and the refractive index at the edge of the lens. The smaller the thickness, the lower is the response time and the greater is the materials savings. However, larger thicknesses are required if applications require large focal tunability ranges with short focal lengths. This condition can also be achieved using higher birefringence materials, which enable the use of thinner devices. Once a LC mixture has been selected, the birefringence can be determined as a function of the external voltage by experiments or simulations based on the Frank-Oseen equations. The threshold voltage (V_{th}) is related to the voltage at the lens center, and the saturation voltage (V_{sat}) is related to the voltage at the edge of the lens (2). Exceeding the voltage limits can result in various undesirable effects, such as flatness in the lens center or shrinkage at the lens edges. Next, we estimate the parameter $\alpha = V_{th}/V_{sat}$, which quantifies the voltage gradient for a proper phase profile. Equation 7 can be evaluated to determine whether a high resistivity layer can be used (the thickness and the diameter are free parameters): the resistance of this layer, if required, can be estimated using (4). If this layer cannot be used, (8) must be considered (in this case, only the thickness or diameter is arbitrary). The simulations or the approximation commented above, can be used to determine the permittivity both vertical and horizontal. If all of the corresponding equations have been satisfied, the resulting lens will have a parabolic phase profile without any of the aforementioned defects.

IV. Experimental Results

A specific application was chosen to validate the developed protocol: a LC-based autostereoscopic display for a mobile application. A commercial nematic liquid crystal MDA-98-1602 from Merck was selected for its high birefringence, $\Delta n = 0.2666$, $\Delta\varepsilon = 12$ ($\varepsilon_o = 4.3$). Two types of devices were designed and manufactured for the study: a monopixel cell and a LC lenticular array. The birefringence was measured using spectroscopy for the monopixel cell and compared to simulation results (Fig. 4). The Kerr effect (which is also known as the quadratic electro-optic

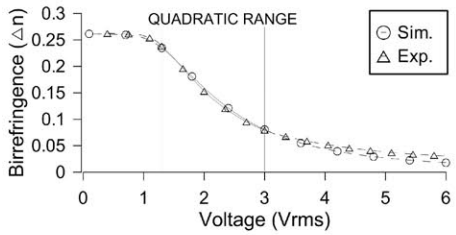

Fig. 4. Experimental and simulated birefringences at 588nm.

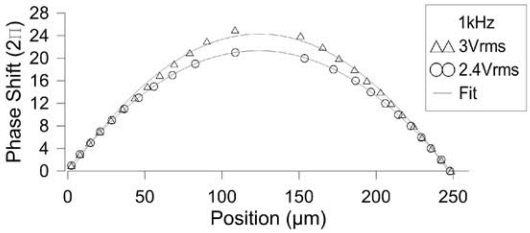

Fig. 5. Experimental phase shift profile and parabolic fit.

effect) was observed for both the experimental and simulated birefringence results from approximately 1.3Vrms to 3Vrms. The protocol requires that $\alpha = 2.3$ to avoid undesirable effects.

To satisfy the requirements of the autostereoscopic application, a cylindrical lens array consisting of 254-μm diameter lenses (for a 200 ppp display) was designed (electrode width = 20 μm, A = 2.1494). For a 3D distance of 25 cm, an interpupilar distance of 65 mm and a pixel pitch of 127 μm, the necessary focal length was 0.48 mm (from geometrical optics [1]). The value of the LC birefringence (in the quadratic range, $\Delta n = 0.1595$) and the focal length determined the LC lens thickness of 105 μm [using (10)]. Thus, following (7), a high resistivity layer can work for a radius greater than $r_{CRIT} = 189$ μm ($\varepsilon'_1 = 12.7$ and $\varepsilon'_2 = 7.9$); that is, lenses with radii of 127 μm did not require modal control. A high resistivity layer was not required for the specifications. Using (8), the ratio between the hole diameter (D = 2r) and the thickness (d) yielded D/d = 2.55, i.e., a resulting thickness of 99.5 μm.

In order to demonstrate these results, a LC lens array was fabricated. A chrome mask consisting of a comb electrode pattern was used for this purpose. We used available materials to manufacture lenses with thickness of 100 μm (using Mylar sheets). The device was electrooptically characterized by analyzing the phase profile generated from the interference pattern. Fig. 5 shows the resulting phase profile of a LC lens with $3V_{rms}$ and $2.4V_{rms}$ of the applied voltage. As it was predicted by the protocol, the phase profile did not show any undesirable effects, such as shrinkage at the lens sides or a plateau in the lens center. For $3V_{rms}$, the maximum quadratic range was achieved using a maximum phase shift of $25 \cdot 2\pi$ rad and a focal length of 0.5 mm (as it was designed). At this focal length, a minimum 3D distance of 25 cm could be achieved. Furthermore, this distance could be tuned by varying the applied voltage: for example, the 3D distance for 2.4 V_{rms} would be 31cm. This experimental result validated the lens design results that were obtained using the analytical approach.

V. Conclusion

We present the first analytical study on the LC microlenses structures. The resulting equations give accurate information about the necessary resistivity for manufacturing modal microlenses. Also, the capacitance provides key information for manufacturing hole patterned lenses. The model was validated for designing lenses with specific parabolic phase profiles and without defects such as shrinkage at the lens sides or a plateau at the lens center. The experimental results are in agreement with the predictions of the equations. The developed method yielded a new protocol for the manufacture of this type of lens. The respective equations are intended to be used as a tool for researchers to produce optimal lenticular designs. The model should result in time savings and maximize material resources, thereby avoiding the manufacture of test cells.

References

[1] V. Urruchi, J. F. Algorri, J. M. Sánchez-Pena, M. A. Geday, X. Q. Arregui, and N. Bennis, "Lenticular arrays based on liquid crystals," *Opto-Electron. Rev.*, vol. 20, no. 3, pp. 260–266, 2012.

[2] J. G. Lu, X. F. Sun, Y. Song, and H. P. D. Shieh, "2-D/3-D switchable display by Fresnel-type LC lens," *J. Display Technol.*, vol. 7, no. 4, pp. 215–219, Apr. 2011.

[3] G. D. Love and A. F. Naumov, "Modal liquid crystal lenses," *Liquid Crystals Today*, vol. 10, no. 2, pp. 1–4, 2000.

[4] H. C. Lin, M. S. Chen, and Y. H. Lin, "A review of electrically tunable focusing liquid crystal lenses," *Trans. Electr. Electron Mater.*, vol. 12, no. 6, pp. 234–240, 2011.

[5] O. Pishnyak, S. Sato, and O. D. Lavrentovich, "Electrically tunable lens based on a dual-frequency nematic liquid crystal," *Appl. Opt.*, vol. 45, pp. 4576–4582, 2006.

[6] O. G. Vendik, S. P. Zubko, and M. A. Nikol'skii, "Modeling and calculation of the capacitance of a planar capacitor containing a ferroelectric thin film," *Tech. Phys.*, vol. 44, no. 4, pp. 349–355, Apr. 1999.

[7] V. Urruchi, J. F. Algorri, C. Marcos, and J. M. Sánchez-Pena, "Electrical modeling and characterization of voltage gradient in liquid crystal microlenses," *Rev. Sci. Instrum.*, vol. 84, no. 11, pp. 116105-1–116105-3, 2013.

[8] M. R. Costa, R. A. C. Altafim, and A. P. Mammana, "Electrical modeling of liquid crystal displays-LCDs," *IEEE Trans. Dielectr. Electr. Insul.*, vol. 13, no. 1, pp. 204–210, Feb. 2006.

[9] V. Urruchi, J. F. Algorri, J. M. Sánchez-Pena, N. Bennis, M. A. Geday, and J. M. Otón, "Electrooptic characterization of tunable cylindrical liquid crystal lenses," *Molecular Cryst. Liquid Cryst.*, vol. 553, no. 1, pp. 211–219, 2012.